

# AUTOMATIC MEASUREMENT ON CT IMAGES FOR PATELLA DISLOCATION DIAGNOSIS

Qi Kong<sup>1</sup>, Shaoshan Wang<sup>2</sup>, Jiushan Yang<sup>2</sup>, Ruiqi Zou<sup>3</sup>, Yan Huang<sup>1†</sup>, Yilong Yin<sup>1</sup>, Jingliang Peng<sup>1</sup>

<sup>1</sup>School of Computer Science and Technology, Shandong University, China

<sup>2</sup>Department of orthopedics, Affiliated hospital of Shandong University of TCM, China

<sup>3</sup>Shandong University of TCM, China

## ABSTRACT

To diagnose the patella dislocation, various angles and distances need to be measured on knee CT images, which was traditionally done by doctors manually. In this work, we propose a novel scheme for automatic measurement on knee CT images to assist doctors diagnosis of patella dislocation. Specifically, we first segment the femur and the patella regions on the CT images, then adopt optimal fitting to obtain the central planes of the femur and the patella bones and, based on which, make the measurement. As experimentally demonstrated, the measured results obtained with our system are highly consistent with those manually made by experienced doctors.

**Index Terms**— patella dislocation, CT image, Image segmentation

## 1. INTRODUCTION

Patellar dislocation occurs when the patella slips out from the patellar surface of femur. It is a common knee injury that may happen when people, especially teenagers and athletes, do vigorous physical exercises, e.g., basketball and football playing. To diagnose the injury, clinical doctors need to measure a set of quantities such as the angles and the distances between the patellas and the femurs central planes. The measurement has been traditionally made manually on the knee CT images, which is usually complex, tedious and error-prone. Moreover, the patients are often required to put their legs at fixed angles when CT scanned to ease the measurement.

As such, it is helpful to build a system for automatic measurement on knee CT images, significantly saving doctors effort in patellar dislocation diagnosis. To the best of our knowledge, no work has been published specifically for this purpose. In this work, we develop a system for automatically measuring key angle and distance parameters on knee CT images which serve as the basis of doctors diagnosis of patellar dislocation. With the help of this system, the patients do not have to bend their knees at fixed angles but may move their legs naturally through a range of knee angles; the right CT

images are automatically selected from the input set and the measurements are made automatically on the selected images.

## 2. SYSTEM OVERVIEW

The input to our system is a sequence of CT images scanned on cross sections of the knee region at each time instance, as illustrated in Fig. 1. More specifically, our current system works on CT images of the upper part of the knee region, *i.e.*, CT images that contain the cross sections of both the femur and the patellar, as illustrated in the right column of Fig. 1.

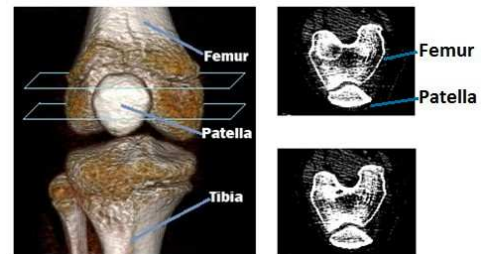


Fig. 1. Examples of knee CT images.

For an input CT image set taken at each time instance, the measurement process works in three steps, as illustrated in Fig. 2: (1) for each CT image, we delineate the main region of bones, (2) we select the set of CT images with well-identified femur and patella regions, (3) we compute the central axial planes for the femur and the patella, respectively, for use in measurement.

## 3. ALGORITHMS

Taking advantage of the a priori knowledge that each CT image contains exactly two meaningful regions (corresponding to femur and patella) and their positions and shapes vary only slightly between adjacent CT images, we design algorithms that satisfactorily serve our purpose.

†: Corresponding author (Email: yan.h@sdu.edu.cn).

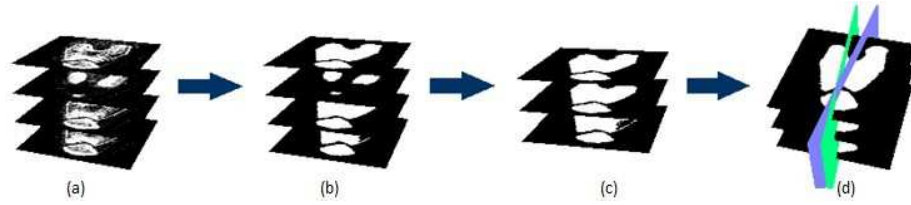


**Fig. 2.** Illustration of the measurement process: (1) input CT images, (b) major bone region delineation, (c) bad result elimination, and (d) angle and distance measurement.

### 3.1. Femur and Patella Delineation

Delineation of the femur and the patella regions in a CT image is difficult due to the following characteristics of the knee CT images: (1) a CT image simultaneously contains responses of bones, soft tissues and noises; (2) the patella and the femur regions are very close to each other (*e.g.*, only one or two pixels apart) in many CT images.

The problem of femur and patella delineation is in essence a segmentation problem. The image segmentation problem has been extensively researched and typical methods include thresholding methods [1], morphological methods [2, 3] and region-based active contour methods [4, 5]. Thresholding methods are simple but it is often hard to choose the right thresholds for a clear segmentation; morphological methods are flexible but may deform the image; region-based active contours methods often work better but are sensitive to noise in the image.

Directly running the active contour algorithm on the CT image may not give accurate results, as shown in Fig. 3(a), due to the effect of soft tissue and noise pixels and the close distance between the femur and the patella regions. In order to suppress the effect of those soft tissue and noise pixels, we propose to enhance the contrast of the original images by increasing the bone tissue pixels' gray levels while decreasing the soft tissue and noise pixels' gray levels. In order to clearly separate the femur and patella regions, we further detect a connected background path between the two regions and set the gray levels of the pixels along that path as black. Thereafter, we run the region-based active contour algorithm on the pre-processed image to obtain the final segmentation.

#### 3.1.1. Contrast Enhancement

The common global contrast enhancement method based on histogram manipulation does not work well for our case. The reason is that the pixels' gray levels concentrate around very low and very high values (see Fig. 4), leaving little room for contrast enhancement. Instead, we propose a contrast enhancement method based on local characteristics around each pixel. Observing that higher (lower) gray levels correspond to bone tissues (soft tissues and probably noise), we increase (decrease) the gray level of a pixel with brighter (darker)

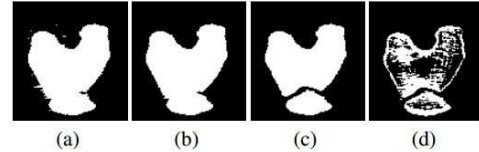


**Fig. 3.** Various results for an exemplar CT image: (a) region-based active contour, (b) contrast enhancement plus region-based active contour, (c) contrast enhancement, separating path detection plus region-based active contour and (d) binarized version of the original image.

neighborhood.

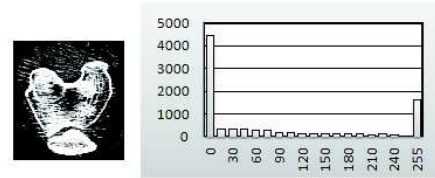


**Fig. 4.** Histogram of a knee CT image. We can see the pixels gray levels concentrate around very low and very high values.

Specifically, we perform a nonlinear scaling of each pixel's gray level according to its neighboring pixels' gray levels. For a pixel,  $p_0$ , we denote its gray level as  $g_0$  and the gray levels of all the other pixels in  $p_0$ 's  $3 \times 3$  neighborhood as  $g_i$  ( $i \in 1, 2, \dots, 8$ ). Assuming that the maximum gray level is 255, we update  $g_0$  to  $g'_0$  according to

$$g'_0 = g_0 \times e^{\alpha - 0.45}$$

where

$$\alpha = \frac{\sum_{i=0}^8 g_i}{255 \times 9}$$

We found by experiments that the above process, when iterated for more than one pass, yields better results. Comparing Fig. 3(b) and Fig. 3(a), we observe an obviously improved result with the gray level enhancement technique.

### 3.1.2. Separating Path Detection

Though the proposed contrast enhancement algorithm improves the segmentation results, when the femur and the patella regions are very close to each other, they may still be recognized as one region by the active contour algorithm, as shown in Fig. 3(b). In order to separate the femur and the patella regions, we propose to first detect a connected path on the background which clearly separates the two regions and then explicitly set the pixels covered by this path as background pixels (*i.e.*, black pixels) in the original CT image.

We propose a graph-based separating path detection algorithm that works on the binarized CT image. Given a CT image, we first binarize it with 1-valued pixels roughly corresponding to the bone tissues and 0-valued pixels the soft tissues and the background. A high threshold for the binarization is used in our experiments to make an aggressive separation of the femur and the patella regions. Note that the binary image itself does not readily give an accurate segmentation of the CT image, as shown in Fig. 3(d).

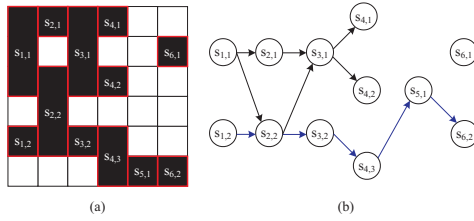


**Fig. 5.** An example of binarized image is shown in (a) and its segment graph is constructed in (b) where the blue arrows illustrate the detected path.

Assume that the resolution of the CT image is  $M \times N$ . For the  $i$ -th ( $i \in \{1, 2, \dots, N\}$ ) column of the binarized image, we identify the  $k_i$  continuous segments of black pixels on it and represent each with a node,  $s_{i,j}$  ( $j \in \{1, 2, \dots, k_i\}$ ) in a graph,  $G$ . If a segment,  $s_{i,s}$  ( $1 \leq s \leq k_i, 1 \leq i < N$ ), in the  $i$ -th column is connected to a segment,  $s_{i+1,t}$  ( $1 \leq t \leq k_{i+1}$ ), we add a directed edge  $(s_{i,s}, s_{i+1,t})$  in  $G$ . An example is given in Fig. 5, where the continuous black segments on each column are labelled on the original binarized image as shown in Fig. 5(a) and the correspondingly constructed graph is given in Fig. 5(b).

Thereafter, starting from each node,  $s_{1,j}$  ( $1 \leq j \leq k_1$ ), we conduct a depth-first traversal in the directed graph. During the traversal, whenever we reach a node,  $s_{N,l}$  ( $1 \leq l \leq k_N$ ), we have retrieved a connected path going from the first column to the last of the image. As illustrated with blue arrows in Fig. 5(b).

In rare cases, we may obtain more than one connected paths and select the right one based on the fact that the right path usually has small variation in curvature and width going

from the left to the right. Comparing Fig. 6(c) with Fig. 6(b), we clearly see the effect of the separating path detection.



**Fig. 6.** Bad results should be eliminated after the segmentation, which do not give right shapes for the femur and the patella. Erroneous cases include (a) one big major region and (b) more than two major regions.

### 3.2. Angle and Distance Measurement

In a segmented CT image, we expect to have two major regions with right shapes, corresponding to the femur and the patella, respectively. However, it may happen that there are more or less than two major regions in the segmented image, as illustrated in Fig. 6. We simply discard those CT images and do not use them for measurement.

Two key parameters are often measured by doctors in patella dislocation diagnosis: the angle and the distance between the femur's central plane and the patella's central plane. Therefore, to make these measurements, we first need to compute the central planes of the femur and the patella.

The CT images are acquired on parallel cross sections of the knee region, as shown in Fig. 1. As such, we locate a few key points on each CT image in the central area of the femur region and the patellar region, respectively, and then compute the central planes for the femur and the patella bones by optimally fitting those key points on the CT images.

#### 3.2.1. Key Point Selection

Our system automatically selects the key points for the femur and the patella regions based on the following criteria. For the femur region in each CT image, we select three points as the key points: the two central valley points along the boundary and the middle of the leftmost and the rightmost points. The key points for the patella region in each CT image are selected in the same way. This key point selection scheme is illustrated in Fig. 7.

#### 3.2.2. Plane Fitting

The central plane of the femur bone is acquired by optimally fitting a plane to the femur's key points on the CT images. Similarly, the central plane of the patella bone is acquired by optimally fitting a plane to the patella's key points.



**Fig. 7.** Every bone has three automatically selected key points: two central valley points along the boundary and the middle of the leftmost and the rightmost points, as colored red and green in the figure.

In general, denoting the points as  $p_i(x_i, y_i, z_i)$  ( $i = 1, 2, \dots, K$ ) and the plane equation as  $z = ax + by + c$ , the plane that optimally fits those points can be obtained by

$$\min_{a,b,c} \sum_{i=1}^K (z_i - ax_i - by_i - c)^2$$

which can be solved with the method of least square error.

### 3.2.3. Angle and Distance Measurement

We first measure the angle,  $\theta$ , between the femur's and the patella's central planes by computing the angle between their normals. If  $\theta$  is above a threshold,  $T_\theta$ , patella dislocation is detected. Otherwise, we perform further distance measurement as described below, which will provide doctors with valuable parameters for further diagnosis.

We fit a pair of parallel planes to the femur's and the patella's key points, respectively, and measure the distance,  $D$ , between the two parallel planes. Assuming that the equations of the two planes are  $z = ax + by + c_1$  and  $z = ax + by + c_2$ , given the femur's key points as  $p_i(x_i, y_i, z_i)$  ( $i = 1, 2, \dots, K$ ), and the patella's key points as  $p'_i(x'_i, y'_i, z'_i)$  ( $i = 1, 2, \dots, K$ ), the parallel plane fitting is done by

$$\min_{a,b,c_1,c_2} \sum_{i=1}^K (z_i - ax_i - by_i - c_1)^2 + (z'_i - ax'_i - by'_i - c_2)^2$$

again using the method of least square error.

## 4. EXPERIMENTAL RESULTS

We experiment on three patients dynamic knee CT data. For each patient, we ask him/her to move his/her legs freely from 0 degree to about 90 degrees while being scanned. We pick up the CT images taken at four random time instances,  $T_1$ ,  $T_2$ ,  $T_3$  and  $T_4$ , for experiments. For the CT image set at each time instance, we use our system to automatically measure the angle,  $\theta$ , and the distance,  $D$ . Note that when  $\theta > 10$ , we do not measure the  $D$ . For the purpose of comparison, we ask an experienced doctor to measure the same parameters on the CT images manually. We use the unit of degree for angle measurement and the unit of millimeter for distance measurement.

Note that, for the automatic measurement, we have converted the unit of pixel to the unit of millimeter, knowing that one pixel corresponds to 10 millimeters in the photographing. All the experimental data are given in Table 1. From Table 1, we see that there is very little difference between the automatically and manually measured angle numbers. Similarly, the automatically and the manually measured distances also closely match each other, as can be observed from Table. 1 .

**Table 1.** Measurement result of our method and manual method.

| Patients  | Type     | Methods   | $T_1$ | $T_2$ | $T_3$ | $T_4$ |
|-----------|----------|-----------|-------|-------|-------|-------|
| Patient#1 | Angle    | Automatic | 2.4   | 4.6   | 1.4   | 2.0   |
|           |          | Manual    | 2     | 4.5   | 1.5   | 2     |
|           | Distance | Automatic | 0.6   | 0.8   | 0.6   | 0.3   |
|           |          | Manual    | 0.5   | 0.7   | 0.6   | 0.3   |
| Patient#2 | Angle    | Automatic | 11.6  | 4.4   | 5.6   | 9.5   |
|           |          | Manual    | 12    | 4     | 6     | 10    |
|           | Distance | Automatic | /     | 2.2   | 3.5   | /     |
|           |          | Manual    | /     | 2.0   | 3.2   | /     |
| Patient#3 | Angle    | Automatic | 2.8   | 1.6   | 2.8   | 3.3   |
|           |          | Manual    | 3     | 2     | 3     | 3     |
|           | Distance | Automatic | 0.4   | 0.8   | 0.6   | 0.5   |
|           |          | Manual    | 0.4   | 0.7   | 0.6   | 0.6   |

## 5. CONCLUSION

In this work, we develop a system for automatic measurement of certain distance and angle quantities on knee CT images. We propose novel algorithms to segment the femur and patella regions in the CT images, which is a difficult task using generic image segmentation algorithms. In addition, we propose to use optimal fitting method to obtain the central planes of the bones and, based on which, to perform the measurement. The measurement results obtained with the proposed system are highly consistent with those made manually by experienced doctors.

In the future, we will extend our system to measure more parameters as needed by doctors. Furthermore, we will investigate measuring on the reconstructed 3D volume with more flexibility.

## Acknowledgement

This work was supported by the Scientific Research Foundation for the Excellent Middle-Aged and Youth Scientists of Shandong Province of China (Grants No. BS2011DX017), NSFC Joint Fund with Guangdong under Key Project (Grants No. U1201258), the National Natural Science Foundation of China (Grants No. 61070103 and No. U1035004), the Program for New Century Excellent Talents in University (NCET) in China and Shandong Provincial Natural Science Foundation, China (Grants No. ZR2011FZ004).

## 6. REFERENCES

- [1] Zhi-Jia Zhang, "Improved multi-threshold image segmentation algorithm based on potential function clustering," *Opto-Electronic Engineering*, vol. 32, no. 8, pp. 64–68, 2005.
- [2] P. Soille, *Morphological Image Analysis: Principles and Applications*, Springer, 1999.
- [3] Frédéric Zana and Jean-Claude Klein, "Segmentation of vessel-like patterns using mathematical morphology and curvature evaluation," *IEEE Transactions on Image Processing*, vol. 10, no. 7, 2001.
- [4] Ronfard R., "Region-based strategies for active contour models," *International Journal of Computer Vision*, vol. 13, no. 2, pp. 229–251, 1994.
- [5] F. Derraz, A. Taleb-Ahmed, and A. Chikh, "Improved edge map of geometrical active contour model based on coupling to anisotropic diffusion filtering," *Bioinformatics and Bioengineering*, vol. 10, pp. 1097–1101, 2007.